Methane internal reforming in solid oxide fuel cells with anode off-gas recirculation

Tsai, Tsang-I; Troskialina, Lina; Majewski, Artur; Steinberger-Wilckens, Robert

DOI:
10.1016/j.ijhydene.2015.10.025

Document Version
Early version, also known as pre-print

Citation for published version (Harvard):
Tsai, T-I, Troskialina, L, Majewski, A & Steinberger-Wilckens, R 2016, 'Methane internal reforming in solid oxide fuel cells with anode off-gas recirculation', International Journal of Hydrogen Energy, vol. 41, no. 1, pp. 553–561. https://doi.org/10.1016/j.ijhydene.2015.10.025

Elsevier Editorial System(tm) for
International Journal of Hydrogen Energy
Manuscript Draft

Manuscript Number: HE-D-15-01642R1

Title: Methane Internal Reforming in Solid Oxide Fuel Cells with Anode Off-Gas Recirculation

Article Type: Full Length Article

Section/Category: Fuel Cells & Applications

Keywords: methane steam reforming; methane dry reforming; carbon deposition; thermodynamic equilibrium; solid oxide fuel cell; SOFC; anode off-gas recirculation

Corresponding Author: Prof. Robert Steinberger-Wilckens, Prof.Dr.

Corresponding Author's Institution: University of Birmingham

First Author: TSANG-I TSAI

Order of Authors: TSANG-I TSAI; Lina Troskialina; Artur Majewski; Robert Steinberger-Wilckens

Abstract: In this study, methane steam and dry reforming have been investigated, from the perspective of methane conversion, hydrogen yield and the formation of solid carbon. Different ratios between methane, steam and carbon dioxide were used in order to simulate the methane internal reforming in a Solid Oxide Fuel Cell (SOFC) with anode off-gas recirculation. Thermodynamic equilibrium modelling was first employed to determine the concentrations of each gas in the equilibrium state. Crushed anode substrate material of a commercial SOFC half-cell was used as catalyst in the practical experiments. The modelling results showed that at 750℃ (1023K), above 90% of methane conversion was found in all cases and carbon was formed when the oxygen to carbon (O/C) ratio was lower than 1.2. The experimental results showed that poor methane conversion rates (around 20%) were found within the steam reforming. The performance was highly affected by the total fuel flow rate and carbon formation could still be found in cases for the O/C ratio above 1.5.

Methane Internal Reforming in Solid Oxide Fuel Cells with Anode Off-Gas Recirculation

T.-I Tsai, L. Troskialina, A. Majewski and R. Steinberger-Wilckens*
School of Chemical Engineering, University of Birmingham,
Edgbaston, Birmingham, B15 2TT, U.K.

Corresponding author: Tel:+44 (0) 121 415 8169

Email:R.STEINBERGERWILCKENS@BHAM.AC.UK

Abstract

In this study, methane steam and dry reforming have been investigated, from the perspective of methane conversion, hydrogen yield and the formation of solid carbon. Different ratios between methane, steam and carbon dioxide were used in order to simulate the methane internal reforming in a Solid Oxide Fuel Cell (SOFC) with anode off-gas recirculation. Thermodynamic equilibrium modelling was first employed to determine the concentrations of each gas in the equilibrium state. Crushed anode substrate material of a commercial SOFC half-cell was used as catalyst in the practical experiments. The modelling results showed that at 750℃ (1023K), above 90% of methane conversion was found in all cases and carbon was formed when the oxygen to carbon (O/C) ratio was lower than 1.2. The experimental results showed that poor methane conversion rates (around 20%) were found within the steam reforming. The performance was highly affected by the total fuel flow rate and carbon formation could still be found in cases for the O/C ratio above 1.5.

Keywords: *methane steam reforming, methane dry reforming, carbon deposition, thermodynamic equilibrium, solid oxide fuel cell, anode off-gas recirculation*

1. Introduction

In solid oxide fuel cells (SOFCs), hydrocarbons can be directly reformed into hydrogen-rich gases inside the cell due to their high operating temperature [1]. Additionally, the energy required for the strongly endothermic reforming reactions can be derived from the heat generated inside the cell. Natural gas, for example, which mainly consists of methane, is a prime choice of fuel for SOFCs employed as residential combined heat and power units (microCHP) due to the well established natural gas distribution infrastructure in households. SOFCs running on natural gas can be applied widely for both μCHP and decentralised generation (DG) in the drive to

reducing electricity transmission losses and increasing the efficiency of electricity supply.

Two methods are regularly used for converting methane into hydrogen-rich gases: steam methane reforming (SMR, Equation 1) and dry methane reforming (DR, Equation 2) [2].

$$CH_4 + 2H_2O \leftrightarrow CO_2 + 4H_2 \quad \text{Equation 1}$$

$$CH_4 + CO_2 \leftrightarrow 2CO + 2H_2 \quad \text{Equation 2}$$

However, solid carbon can be formed during the reforming process through methane cracking (MC, Equation 3) and the Boudouard reaction (BD, Equation 4). The carbon deposited will increasingly reduce the porosity in the anode and cover the nickel catalyst thus lowering the performance.

$$CH_4 \leftrightarrow C + 2H_2 \quad \text{Equation 3}$$

$$2CO \leftrightarrow C + CO_2 \quad \text{Equation 4}$$

In order to overcome this problem, additional H_2O or CO_2 needs to be added to the fuel, lowering the concentrations of CH_4 or CO from the SMR or water gas shift reactions (WGS, Equation 5).The formed solid carbon, though, can theoretically be removed by syngas formation (SF, Equation 6).

$$CO + H_2O \leftrightarrow CO_2 + H_2 \quad \text{Equation 5}$$

$$C + H_2O \leftrightarrow CO + H_2 \quad \text{Equation 6}$$

Both CO_2 and H_2O can be found in the SOFC anode exhaust as they are the products of CO and H_2 oxidation. As a result, anode off-gas recirculation (AOGR) is an option to be applied in SOFC μCHP and DG systems, where the addition of purified water or carbon dioxide are undesired since they increase the system complexity and the requirements for maintenance. Moreover, the fuel cell system can further benefit from the exhaust gas recycling since the returned gas has a similar temperature as the cell, and thermal gradients can be prevented without or with reduced requirements on a pre-heater.

On the other hand, a more complex reaction system is formed due to the competition between H_2O and CO_2 for reacting with methane.Also, a lower system performance results from the lower fuel partial pressure due to the introduced non-fuel gases. As a

result, a detailed inspection of the interaction among CH_4, H_2O and, CO_2 is required for a more in-depth investigation.

A study of methane dry reforming from the point of view of thermodynamics was carried out by Nikoo and Amin [3]. Al-Nakoua et al [4] reported, that the combined methane steam and dry reforming had the ability to improve the catalyst stability, but the carbon formation and ratios among the reactants were less addressed. Kinetic modelling work was carried out by Maestri [5]. The conclusion that the water concentration could have a significant effect on the combined methane reforming was obtained by Soria et al [6]; however, the carbon dioxide concentration was fixed in their experiments. A nickel-silica core@shell catalyst used for methane tri-reforming was reported by Majewski and Wood [7]. Research towards methane internal reforming with gold doped Ni/GDC was carried out by Niakolas et al. [8], which resulted in a higher tolerance to carbon formation; however, the amount of gold needs a further investigation. Goula et al. [9] investigated the methane internal reforming with a Ni based anode from the catalyst and electrocatalytic point of view. Their results suggest that a closed-circuit operating SOFC could operate stably for an extended period of time due to the carbon electro-oxidation reactions. A similar result was obtained by Lin et al. [10], who suggests that the current density has a strong effect on carbon formation. This is particularly obvious when pure methane is used as fuel and the temperature is below 700 ℃. Oyama et al. [11] report that the methane dry reforming performs less efficient than steam reforming since the produced hydrogen can be consumed with carbon dioxide through the reversed WGS reaction. Additionally, a higher hydrogen yield can be obtained by steam reforming as the produced carbon monoxide (reacting with water) boosts the hydrogen yield. An investigation towards SOFC direct internal reforming of biogas was conducted by Lanzini and Leone [12]. The results suggested that a SOFC running on biogas without degradation is possible when the correct amount of oxidant is added, which is also agreed by Shiratori et al. [13]. The later ones suggested that the ratio of 1.5 between methane and carbon dioxide can enhance the electrochemical consumption of methane. A kinetic equation of hydrogen yield was derived and then verified by Fan et al. [14] when Ni-Co/MgO-ZrO_2 is used as the catalyst for the dry reforming of methane. Some dynamic modelling work relating to the control aspects were carried out by Görgün et. al [15], Varigonda and Kamat [16], and Pukrushpan et. al [17]. In these three papers, the chemical reactions were considered from a kinetic viewpoint and the heat management was also included. A controller could be designed based on these modelling resutls.

In this study, combined methane steam and dry reforming was investigated, from both

thermodynamic equilibrium modelling and experiments. The aim of this work was to find the interactions among the reforming reactions, carbon formation, and the ratio among the reactants.

2. Experiments

2.1 Modelling

The National Aeronautics and Space Administration (NASA) Chemical Equilibrium with Applications (CEA) was employed to carry out the thermodynamic equilibrium calculations. In this software, the concentrations at equilibrium are obtained based on the minimised Gibbs free energy from a variety of initial conditions [18]. The reforming product compositions are not affected by the catalyst material and particle size used in the experiment. The reforming results can be calculated by the software from the given conditions including the reactants, temperature, pressure and expected products. The equilibrium results are expected to relate to the long-term operation of an SOFC system.

2.2 Experimental Study

2.2.1 Catalyst Preparation and Characterisation

A commercial anode-supported SOFC half cell that consisted of anode and electrolyte was used in this experiment as the catalyst to represent the SOFC internal reforming conditions. These SOFC half-cells were used due to their availability as standardised and commercial components with reproducible properties. They consisted of a 400 μm nickel- Yttria-stabilized zirconia (Ni-YSZ) anode and a 8 to 10 μm thick Yttria-stabilized zirconia electrolyte. This material was chosen because of its facile availability. For the experiments, the electrolyte half-cells were ground into powders to make the nickel accessible to the gas stream, since this is regarded as the catalyst for methane reforming. From the point of view of the reforming experiment, anode substrates would have been sufficient. Nevertheless, the YSZ electrolyte is inert to the reforming reactions and thus did not harm the experiments.

The cells were examined using a Burker S8 Tiger X-Ray Fluorescence (XRF) to determine their composition. Then the Micromeritics Autochem II Chemisorption Analyser was applied for Temperature Programmed Reduction (TPR) to find the proper reduction temperature. In the Temperature programmed reduction, the analysis was conducted on a plain 0.1 g half-cell (anode substrate and electrolyte) in a helium atmosphere and heated at a rate of 10℃ min^{-1} from room temperature to 500℃, then cooled down to 25℃. This stage was employed to remove the impurities. The sample was then heated up again at the same rate to 750℃ under an atmosphere consisting of

10% hydrogen and 90% helium. The reduction process was monitored from the thermal conductivity detector signal.

An amount of 0.2 g of the cell was ground into particles with diameters smaller than 600 μm. This powder was then mixed with 1.8 g silicon carbide (SiC) to form the catalyst bed and placed in the centre of the reaction tube with quartz wool stuffed at both ends. SiC was selected due to its high heat and wear resistance, and its chemical inertness to all alkalis and acids. The mix of SiC and catalyst was used to allow the system to behave more isothermally and to avoid gas pressure drops, particle clogging, and catalytic bypassing. This procedure is commonly used for testing a sample of a catalyst in a fixed bed reactor. The pure SiC at the gas entrance was used to distribute and heat up the fuel flow to allow homogenous reaction conditions, and the pure SiC at the gas exit was used to support the whole catalyst bed. Glass wool was placed as additional support, as shown in Figure 1. The whole tube was then placed in the centre of a tubular furnace. The gas flow rate was controlled by Brooks 5850S Mass Flow Controllers (MFCs). After cooling and water condensation the exhaust was connected to an on-line Agilent Technologies 7890A Gas Chromatograph (GC) to examine the reformed gas, as shown in Figure 2.

<Fig. 1 near here>

<Fig. 2 near here>

Prior to the reforming reactions, the catalyst was heated to 200℃ at a rate of 20℃ min^{-1}, with 10 sccm of hydrogen flow. The heating rate was then decreased down to 5 ℃ min^{-1} until the system reached 750℃ (1023 K). Slowing of the heating rate was used to prevent the aggregation of nickel. The system was kept for 1 hour at 750 ℃ and 10 sccm hydrogen flow to allow the nickel to be fully reduced. After that, 100 sccm of helium was given for 5 minutes before the reforming started.

2.2.2 Reforming Reaction

The parameters of the gas flow used in the experiments are listed in Table 1. Case 3 was not experimentally tested because the modelling results had shown good abilities in methane conversion and no carbon formation. The O/C ratio was defined as the atomic ratio between oxygen and carbon in the inlet fuel stream, which ratio will also be used in the further discussion. Water was added in liquid form through a pump with a range between 0-0.04 g min^{-1} to represent 0-50 sccm of steam flow rate and then heated up to 120℃ in a pre-heater before mixing with the other gases. Helium or

other inert gases were not added to unify the total fuel flow rate in each case. This is because the total flow highly depends on the recycling rate in the SOFC AOGR. Moreover, the composition of the anode exhaust is affected by the cell operating status. The total flow rate is thus not consistent under the different conditions.

Table 1 Parameters of methane reforming reactants.

	CH_4 (sccm)	H_2O (g min^{-1})	CO_2 (sccm)	O/C ratio
Case 1	25	0.02	0	1
Case 2	25	0.03	0	1.5
Case 3	25	0.04	0	2
Case 4	25	0	25	1
Case 5	25	0	37.5	1.2
Case 6	25	0	50	1.333
Case 7	50	0.04	50	1.5
Case 8	25	0.02	25	1.5
Case 9	25	0.04	50	2
Case 10	25	0.02	37.5	1.6
Case 11	25	0.03	25	1.75

2.2.3 Carbon Deposition

Thermogravimetric analysis

Thermogravimetric analysis (TGA) was used to examine the solid carbon formed from the reforming reactions. The sample is heated in a constant air flow, and as the temperature increases, carbon is oxidised and forms carbon dioxide gas which escapes into the atmosphere, thus reducing the weight of the sample. In the experiment, a NETZSCH TG209F was employed to examine the carbon in the sample. In this analysis, the used half-cell catalyst was first separated from the mixture with SiC, and then a small amount (around 25 mg) was used for the analysis.

However, the metallic nickel was also oxidised in the analysis. This also led to further weight increase. In order to remove this influence, the same amount of unused catalyst was reduced and then oxidised to measure the weight change attributed to oxidation of nickel. That sample was used as a reference to the spent catalyst to calculate the carbon deposition. For the reduction, the sample was heated up from room temperature to 1000℃ at a rate of 10℃ min^{-1} with a hydrogen flow rate of 40 sccm. The results are shown in Figure 7 and will be discussed below.

The samples for the oxidation process were heated up at 20℃ min^{-1} to 900℃ with 40 sccm of air flow. The weight change in percentage against the reference was then

turned into the numerical data, for comparison with the Temperature Programmed Oxidation (TPO) results.

Temperature Programmed Oxidation

The amount of 1 g of the catalyst bed (mixture of catalyst and SiC) used in the methane reforming experiment was placed in the centre of a quartz tube inside a furnace, as shown in Figure 3. The exhaust from the tube was connected to an on-line MKS minilab LM80 Mass spectrometer (MS). A mixture of gas consisting of 40 sccm helium and 10 sccm oxygen was fed at room temperature for 1 hour to remove the impurities. The tube was then heated up with the same gas condition at a rate of 10℃ min^{-1} to 900℃ and kept for 30 minutes or longer until no carbon dioxide signal was observed anymore in the MS. This allowed the solid carbon formed from the reforming experiment to be oxidised into carbon dioxide gas and then detected by the MS connected at the exhaust. The tube was then cooled down naturally under a 50 sccm helium gas flow. The catalyst bed was separated into SiC and the ground half-cell catalyst, for which the weight was used to work out the amount of carbon formed per gram of the catalyst, reasonably assuming that no carbon was formed on the SiC.

<Fig. 3 near here>

The total amount of carbon dioxide generated during the oxidation of the spent catalyst was calculated by summing all the carbon dioxide signals from the MS during the TPO. Signals from carbon dioxide 25 minutes before and after the peak, respectively, were added and used for further calculation.

2.3 Performance Evaluation

The study aimed at investigating the methane internal reforming in an SOFC with anode off-gas recirculation. For SOFCs, the cell performance highly depends on the hydrogen partial pressure. Despite methane can be theoretically directly oxidised fully or partially to generate electricity [19], the reaction speed is much slower than with the SMR and WGS reactions [20, 21]. Moreover, Ni et al. [22] also pointed out that the WGS reaction speed is much faster than the carbon monoxide oxidation. As a result, the methane conversion and hydrogen yield were the two indicators for examining the reforming performance in this study. The conversion and yield rates were defined as following [23, 24].

$$\text{Methane conversion} = \frac{\upsilon_{CH_4,in} - \upsilon_{CH_4,out}}{\upsilon_{CH_4,in}} \quad \text{Equation 7}$$

$$\text{Hydrogen yield} = \frac{\upsilon_{H_2,out}}{\upsilon_{CH_4,in}} \quad \text{Equation 8}$$

The term υ_i (i =CH_4, H_2) represents the mole flow rate of the two species, respectively.

3. Results and Discussion

3.1 Modelling

Figure 4(a) and (b) present the results from thermodynamic modelling. The residual water and formed solid carbon were included in Figure 4 (a), and excluded in Figure 4(b), which was then used to compare with the experimental results. At 750℃, carbon was formed in the cases 1, 4, and 5 (steam reforming, H_2O:CH_4 = 1; dry reforming, CO_2:CH_4 = 1 and 1.5), when the O/C ratio was below 1.2. All the remaining cases were free from the formation of carbon.

Steam Reforming of Methane

For the methane steam reforming (cases 1, 2, and 3 in Table 1), the hydrogen concentration decreased, from 69% down to 63%, with the increase of the steam to methane (S/C) ratio, as shown in Figure 4(a). This is due to the higher residual steam concentration left from the higher steam input. This can be seen from Figure 4(b): when the water is removed, the hydrogen concentration increases from 72% to 75%. In general, the methane conversion improves with a higher S/C ratio.

Dry Reforming of Methane

For methane dry reforming (cases 4, 5, and 6 in Table 1), the hydrogen concentrations (45%, 38%, and 33%) are significantly lower than the concentrations in steam reforming, as shown in Figure 4(a). Moreover, the hydrogen concentration decreases with the increase in carbon dioxide to methane ratio, even though the methane was converted more completely (Figure 4(b)). This is because unlike water, which contains one molecule of hydrogen, carbon dioxide in dry reforming does not contain additional hydrogen to be released during the reforming reactions. The higher residual carbon dioxide concentration lowers the concentration of other gases. The results from case 6 correspond to the report from Santarelli et al.[25], in which their modelling results showed 31.3%, 21.1% and 17.5% in molar fraction of hydrogen, carbon monoxide and carbon dioxide, respectively, when the CO_2/biogas ratio is set to be 1.0. This case has an O/C ratio of 2.33, and this is the reason why it is compared

with the case 6 in from this work.

The Effect of Flow Rate

Cases 7 and 8 are used to examine how the fuel flow rate affects the reforming performance. The ratios among methane, steam and carbon dioxide are kept the same in both cases (2:2:2 and 1:1:1). However, the thermodynamic equilibrium minimises the Gibbs free energy thus is only affected by the ratios among the reactants. As a result, the concentrations of all species at equilibrium are identical in both cases, as shown in Figure 4(a) and (b).

Combined Steam and Dry Reforming of Methane

Cases 9, 10, and 11 represent the combined methane steam and dry reforming (shown in Table 1). Case 9 has the lowest hydrogen partial pressure among these three (34% or 44%). This is due to the higher ratio between carbon dioxide to methane and steam to methane (the value of 2 in each ratio, respectively). The high O/C ratio leads to a more complete conversion of methane (0.08% or 0.11% of residual methane pressure in Figure 4(a) or (b)); meanwhile, this also leads to a higher steam and carbon dioxide residual pressure. This phenomenon is improved in cases 10 and 11, when the ratios are decreased (H_2O:CH_4 = 1.0 and CO_2:CH_4 = 1.5 in case 10, H_2O:CH_4 = 1.5 and CO_2:CH_4 = 1.0 in case 11). However, with the O/C ratio still above 1.5 (1.6 and 1.75, respectively), these two cases still have a good methane conversion (only 0.32% and 0.33% or 0.37% and 0.40% residual methane concentration, Figure 4 (a) and (b)). This is even better than the methane conversion in case 3 (0.52% of residual methane concentration) when the steam to methane ratio and the O/C ratio were 2. And since case 11 has a higher steam to methane ratio (1.5) than the ratio in case 10 (1.0), case 11 displays a higher hydrogen concentration produced (46.97% or 56.20%), as shown in Figure 4(a).

<Fig. 4 near here>

3.2 Practical Experiments

3.2.1 Catalyst Analysis

The XRF spectrum in Figure 5 shows that the catalyst contained 50% nickel, 47% zirconium and 3% yttrium. Oxygen was not selected for examination because the oxygen was removed during the reduction reaction before the reforming experiments. Additionally, nickel was the element used as the catalyst for the reforming, so as a result, the XRF was employed to show the ratio between nickel and other elements.

<Fig. 5 near here>

The TPR results presented in Figure 6 show that the catalyst was almost fully reduced into nickel metal at 750℃, which was the temperature then used to reduce the catalyst to supply full reforming catalytic activity before the reforming reactions started.

<Fig. 6 near here>

Figure 7 shows the mass change of the catalyst during the reduction process. It can be seen that the mass decreased with increase in temperature. The reduction process started at around 350℃. The reduction rate was faster between 550 and 750℃, and then slowed down at temperatures above 800℃. This indicates that the nickel oxide in the catalyst was reduced above 550℃. The reduction reaction was almost completed at 800℃. This result supports the outcome of the TPR analysis shown in Figure 6.

<Fig. 7 near here>

3.2.2 Reforming Performance

Figure 8 presents the methane conversion and the hydrogen yield results from both experiments and modelling. As discussed before, these two results can affect the SOFC performance significantly. The hydrogen yield was based on the hydrogen moles produced per mole of methane, thus can be more than 100% in cases including water feed.

Steam Reforming of Methane

The experimental results (Figure 8) were different from the modelling approach in the case of methane steam reforming. In the experiments, a lower methane conversion rate was obtained with a higher steam to methane ratio. The methane conversion rate was 22% in case 1. This was even worse in case 2 (higher steam to methane ratio), which had only 8% of methane reformed. This was due to three issues. Firstly, the experiments were highly affected by the reaction time. Unlike the thermodynamic equilibrium, which requires unlimited time to be achieved, the gases had limited time to react on the catalyst in the experiments. The short reaction time led to incomplete reactions. This corresponds to the situation in an SOFC cell with a given geometry (gas channel length) and gas flow rate. Secondly, the higher steam partial pressure reduced the methane concentration. Thirdly, water has a relatively high adsorption enthalpy change (88.68 kJ mol^{-1}), compared to methane (-38.28 kJ mol^{-1}), or carbon monoxide (-70.65 kJ mol^{-1}) as pointed out by Xu [26]. This also lowers the reaction rate, leading to a reduced methane conversion, and thus a lower hydrogen yield. The hydrogen yield was 96.7% and 49.6% in the cases 1 and 2, respectively, comparing to

138.5% and 169.6% from the modelling results.

It can be seen from the results that a higher S/C ratio could benefit the methane reforming from the thermodynamic point of view. Nevertheless, in the practical experiment, the high S/C ratios lowered the methane conversion and the higher fuel flow rate decreased the reaction time and also reduced the reforming performance. These findings are also supported by Wang et al. [27].

Dry Reforming of Methane

The experimental results in the cases 4, 5, and 6, reached 59.6%, 72.2%, and 66.6% methane conversion rate, respectively, despite the fact that from equilibrium modelling the methane conversion should reach 96.8%, 97.2% and 98.6%. The methane conversion in case 4 corresponds to the results from Nikoo and Amin [3], in which the methane conversion reached 97.9%. However, this had improved comparing to the steam reforming cases. With a higher carbon dioxide concentration, a better methane conversion rate was obtained. This could be seen from cases 4 and 5. The reason why the rate decreased when the ratio between carbon dioxide and methane was increased to 2 was because of the higher fuel flow rate. The high flow rates diluted the methane concentration and shortened the reaction time and thus reduced the methane conversion rate. However, in general, the hydrogen yield increased, from 133.9% in case 4 to 138.8% and 142.7% in cases 5 and 6, respectively.

<Fig. 8 near here>

A noteworthy issue is the higher hydrogen yields in the experiments than expected from the modelling (87.2 %, 95.5%, and 96.9%, respectively). This was due to the fact that the thermodynamic modelling assumed high conversion of produced hydrogen into water. The mildly exothermic WGS reaction, which is likely to react backwards at this temperature, would be turning the hydrogen produced and the carbon dioxide into carbon monoxide and water. However, as mentioned, the reaction time was limited in the experiment. As a result, the produced hydrogen and other gases flowed into the GC, thus the reverse WGS reaction hardly occurred. On the other hand, the thermodynamic equilibrium calculation would assume full reaction. This can be seen from Figure 9 where the carbon monoxide concentrations from cases 4, 5 and 6 are 37.1%, 41.8% and 35.3% from the experiments, comparing to 41.9%, 49.8%, and 50.2% from the modelling.

The Effect of Flow Rate

Figure 8 shows that the flow rate can affect the reforming performance significantly. The same ratio among methane, carbon dioxide, and water were set in both cases 7 and 8 (2:2:2 and 1:1:1). Despite the fact that concentrations were identical from the thermodynamic equilibrium perspective (98.1% of methane conversion and 144.2% of hydrogen yield, as shown in Figure 8 (b)), the experimental work showed different results. From Figure 8 (a), the methane conversion rate was only 23.3% in case 7. The low methane conversion rate also led to a low hydrogen yield of only 50.43%. This was improved in case 8, when the flow rate of each reactant was halved. With the lower flow rate, the reforming performance was improved significantly. The methane conversion rate was doubled, to 55.1% and the hydrogen yield reached 155.8% in case 8, as in (Figure 8 (a)).

Combined Steam and Dry Reforming of Methane

Cases 9, 10 and 11 constituted the combined methane steam and dry reforming, which were used to investigate the composition between steam and carbon dioxide. With the highest O/C ratio of 2, case 9 achieved the highest methane conversion rate (99.6%) in all cases, from the thermodynamic perspective, as shown in (Figure 8 (b)). On the other hand, in the experiment, a lower methane conversion rate (13.2%) was obtained for this case. This was due to the higher steam partial pressure and fuel flow rate (methane:steam:carbon dioxide = 1:2:2) among the cases 9, 10, and 11. As discussed, steam and high flow rates can hinder the reforming reactions. Case 9 suffered from

these two effects and thus the lowest hydrogen yield (34.9%) among all three cases was obtained.

The low methane conversion rate was improved in cases 10 and 11, when the total flow rate and the steam concentration were decreased, as given in Table 1. The O/C ratio remained at 1.6 and 1.75, respectively. This led to a complete methane conversion in the modelling (98.9% and 98.8%). In the experiments, 54.8% and 52.6% were achieved. However, with the steam added to the system, the conversion rates were still lower than the DR cases 4 (59.65%), 5 (72.2%) and 6 (66.6%), which only had an O/C ratio equal to 1.0, 1.2 and 1.33, respectively. For the same reason, case 11 had a higher hydrogen yield (161.4%) than case 10 (139.1%), even with the same methane conversion rate.

<Fig. 9 near here>

3.2.3 Carbon Deposition

Figure 10 and Table 2 show the carbon formation from the TPO and the TGA analysis. In general, the higher the O/C ratio, the less carbon formed, apart from the case of pure steam reforming (cases 1 to 3). This is obvious in cases 9, 10, and 11, when combined reforming was applied. Cases 9, 10, and 11 had only traces of carbon formed. In general, dry reforming (cases 4 to 6) resulted in higher carbon formation than steam reforming. In SMR, increasing the amount of steam resulted in higher coke deposition. In DR the highest coke deposition was for the O/C ratio of 1.2 (according to TPO and TGA) and 1.0 (according to TGA). Case 5 with O/C ratio 1.2 was optimal for DR from the methane conversion point of view (Figure 8), but catalyst life would be significantly reduced due to significant coke deposition in that case. Additionally, it can also be seen that for pure steam or dry reforming, the higher flow rate lowers the ability in preventing carbon formation. This is due to the limited reaction time for the steam or carbon dioxide to remove the carbon atom from the catalyst. For both dry and steam reforming of methane, the methane molecule firstly cracks down into solid carbon adsorbed on the catalyst and hydrogen in gaseous form. The Langmuir-Hinshelwood-Hougen-Waston theory is often used to describe these reaction steps [28-30]. Then oxygen atoms from water or carbon dioxide are used to remove the solid carbon from the catalyst [31, 32]. As a result, if the flow rate is too high, the oxygen atoms are unable to finish the second step of reforming, which is to remove the solid carbon and thus causes carbon deposition. Additionally, for the same

reason, the high adsorption enthalpy of steam also lowers the ability in preventing carbon formation.

<Fig. 10 near here>

Table 2 The carbon formation results from TPO and TGA

	CH_4 (sccm)	H_2O (g min^{-1})	CO_2 (sccm)	O/C	C TPO mg g-cat^{-1}	C TGA mg g-cat^{-1}
Case 1	25	25	0	1	15.32	17.28
Case 2	25	37.5	0	1.5	17.86	23.32
Case 4	25	0	25	1	18.43216	47.2624
Case 5	25	0	37.5	1.2	46.91586	39.0624
Case 6	25	0	50	1.333	20.95022	1.7514
Case 7	50	50	50	1.5	14.23843	14.0884
Case 8	25	25	25	1.5	5.36282	12.9194
Case 9	25	50	50	2	6.44221	~0
Case 10	25	25	37.5	1.6	N/K	~0
Case 11	25	37.5	25	1.75	N/K	~0

4. Conclusions

4.1 Methane Reforming

It can be seen from the results presented here that a higher O/C ratio leads to a better methane conversion. However, unlike the conclusions from thermodynamic equilibrium calculations, higher steam concentrations lower the reforming ability and the hydrogen yield. The fuel flow rate affects the reforming process significantly as the fuel only has limited time to react on the catalyst.

4.2 Carbon Deposition

From the carbon deposition, the higher O/C ratio provides a better ability to avoid carbon formation. However, the high flow rates limit the reaction time and thus can negatively impact on this ability.

4.3 Summary Conclusions

From both the point of view of hydrogen yield and the prevention of carbon formation, the following can be concluded: The results suggest that steam to methane ratio equal to 1.0 can provide a better performance than the higher ratios in methane steam reforming. On the other hand, a higher carbon dioxide to methane ratio (i.e. 2.0) is

generally suggested for methane dry reforming. Despite the fact that higher carbon dioxide concentrations studied in cases 5, 6 and 10 require additional carbon dioxide which cannot be provided by AOGR, therefore assuming cases that are too extreme for real SOFC operation, in this paper the interaction of the gas composition was more in focus. A low fuel flow rate can also improve the reforming reaction. Finally, a relatively low steam concentration mixed with a relatively high carbon dioxide concentration is expected to optimise the reforming reactions.

The results suggest that more detailed models and measurements of gas composition are needed to evaluate anode off-gas recycling. It is obvious that both the flow regime and the composition determine the degree to which the equilibrium conditions are achieved. In all cases, the equilibrium values, though, did not reflect what was found in the experiment. The grade to which the results differed is one of the main insights gained here. Apparently there are many possibilities to set conditions close to or far away from equilibrium composition.

Full kinetic modelling is suggested for a more detailed investigation of methane reforming, as the reaction time has an important role in the reforming reactions, as well as in-situ measurements of gas composition in AOGR mode.

Acknowledgements

The author would like to acknowledge Professor Joe Wood of the School of Chemical Engineering at University of Birmingham for using his facility to conduct the reforming experiments.

References

[1] Tsai T-I, Du S, Dhir A, Williams AA, Steinberger-Wilckens R. Modelling a Methane Fed Solid Oxide Fuel Cell With Anode Recirculation System. ECS Transactions. 2013;57:2831-9.

[2] Hecht ES, Gupta GK, Zhu H, Dean AM, Kee RJ, Maier L, et al. Methane reforming kinetics within a Ni–YSZ SOFC anode support. Applied Catalysis A: General. 2005;295:40-51.

[3] Nikoo MK, Amin NAS. Thermodynamic analysis of carbon dioxide reforming of methane in view of solid carbon formation. Fuel Processing Technology. 2011;92:678-91.

[4] Al-Nakoua MA, El-Naas MH. Combined steam and dry reforming of methane in

narrow channel reactors. International Journal of Hydrogen Energy. 2012;37:7538-44.
[5] Maestri M, Vlachos DG, Beretta A, Groppi G, Tronconi E. Steam and dry reforming of methane on Rh: Microkinetic analysis and hierarchy of kinetic models. Journal of Catalysis. 2008;259:211-22.
[6] Soria MA, Mateos-Pedrero C, Guerrero-Ruiz A, Rodríguez-Ramos I. Thermodynamic and experimental study of combined dry and steam reforming of methane on Ru/ ZrO2-La2O3 catalyst at low temperature. International Journal of Hydrogen Energy. 2011;36:15212-20.
[7] Majewski AJ, Wood J. Tri-reforming of methane over Ni@SiO2 catalyst. International Journal of Hydrogen Energy. 2014;39:12578-85.
[8] Niakolas DK, Ouweltjes JP, Rietveld G, Dracopoulos V, Neophytides SG. Au-doped Ni/GDC as a new anode for SOFCs operating under rich CH4 internal steam reforming. International Journal of Hydrogen Energy. 2010;35:7898-904.
[9] Goula G, Kiousis V, Nalbandian L, Yentekakis IV. Catalytic and electrocatalytic behavior of Ni-based cermet anodes under internal dry reforming of CH4 + CO2 mixtures in SOFCs. Solid State Ionics. 2006;177:2119-23.
[10] Lin Y, Zhan Z, Liu J, Barnett SA. Direct operation of solid oxide fuel cells with methane fuel. Solid State Ionics. 2005;176:1827-35.
[11] Oyama ST, Hacarlioglu P, Gu Y, Lee D. Dry reforming of methane has no future for hydrogen production: Comparison with steam reforming at high pressure in standard and membrane reactors. International Journal of Hydrogen Energy. 2012;37:10444-50.
[12] Lanzini A, Leone P. Experimental investigation of direct internal reforming of biogas in solid oxide fuel cells. International Journal of Hydrogen Energy. 2010;35:2463-76.
[13] Shiratori Y, Ijichi T, Oshima T, Sasaki K. Internal reforming SOFC running on biogas. International Journal of Hydrogen Energy. 2010;35:7905-12.
[14] Fan M-S, Abdullah AZ, Bhatia S. Hydrogen production from carbon dioxide reforming of methane over Ni–Co/MgO–ZrO2 catalyst: Process optimization. International Journal of Hydrogen Energy. 2011;36:4875-86.
[15] Görgün H, Arcak M, Varigonda S, Bortoff SA. Observer designs for fuel processing reactors in fuel cell power systems. International Journal of Hydrogen Energy. 2005;30:447-57.
[16] Varigonda S, Kamat M. Control of stationary and transportation fuel cell systems: Progress and opportunities. Computers & Chemical Engineering. 2006;30:1735-48.
[17] Pukrushpan J, Stefanopoulou A, Varigonda S, Eborn J, Haugstetter C. Control-oriented model of fuel processor for hydrogen generation in fuel cell

applications. Control Engineering Practice. 2006;14:277-93.
[18] NASA. NASA Chemical Equilibrium with Applications (CEA). In: Snyder CA, editor.: Christopher A. Snyder.
[19] Kendall K, Finnerty CM, Saunders G, Chung JT. Effects of dilution on methane entering an SOFC anode. Journal of Power Sources. 2002;106:323-7.
[20] Ni M. Modeling of SOFC running on partially pre-reformed gas mixture. International Journal of Hydrogen Energy. 2012;37:1731-45.
[21] Takahashi H, Takeguchi T, Yamamoto N, Matsuda M, Kobayashi E, Ueda W. Effect of interaction between Ni and YSZ on coke deposition during steam reforming of methane on Ni/YSZ anode catalysts for an IR-SOFC. Journal of Molecular Catalysis A: Chemical. 2011;350:69-74.
[22] Ni M, Leung DYC, Leung MKH. Electrochemical modeling and parametric study of methane fed solid oxide fuel cells. Energy Conversion and Management. 2009;50:268-78.
[23] Oliveira ELG, Grande CA, Rodrigues AE. Steam methane reforming in a Ni/Al2O3 catalyst: Kinetics and diffusional limitations in extrudates. The Canadian Journal of Chemical Engineering. 2009;87:945-56.
[24] Huang KGJB. Solid oxide fuel cell technology : principles, performance and operations. Cambridge, UK; Boca Raton, FL: Woodhead Pub. ; CRC Press; 2009.
[25] Santarelli M, Quesito F, Novaresio V, Guerra C, Lanzini A, Beretta D. Direct reforming of biogas on Ni-based SOFC anodes: Modelling of heterogeneous reactions and validation with experiments. Journal of Power Sources. 2013;242:405-14.
[26] Xu J, Froment GF. Methane steam reforming, methanation and water-gas shift: I. Intrinsic kinetics. AIChE Journal. 1989;35:88-96.
[27] Wang Y, Yoshiba F, Kawase M, Watanabe T. Performance and effective kinetic models of methane steam reforming over Ni/YSZ anode of planar SOFC. International Journal of Hydrogen Energy. 2009;34:3885-93.
[28] Langmuir I. THE ADSORPTION OF GASES ON PLANE SURFACES OF GLASS, MICA AND PLATINUM. Journal of the American Chemical Society. 1918;40:1361-403.
[29] Hansen JB. Chapter 13 - Direct Reforming Fuel Cells. In: Shekhawat D, Berry JJSA, editors. Fuel Cells. Amsterdam: Elsevier; 2011. p. 409-50.
[30] Szekely J. Gas-Solid Reactions: Elsevier Science; 2012.
[31] Wei J, Iglesia E. Isotopic and kinetic assessment of the mechanism of reactions of CH4 with CO2 or H2O to form synthesis gas and carbon on nickel catalysts. Journal of Catalysis. 2004;224:370-83.
[32] Snoeck JW, Froment GF, Fowles M. Steam/CO2 Reforming of Methane. Carbon Filament Formation by the Boudouard Reaction and Gasification by CO2, by H2, and by Steam: Kinetic Study. Industrial & Engineering Chemistry Research.

2002;41:4252-65.

Figure 1

Click here to download high resolution image

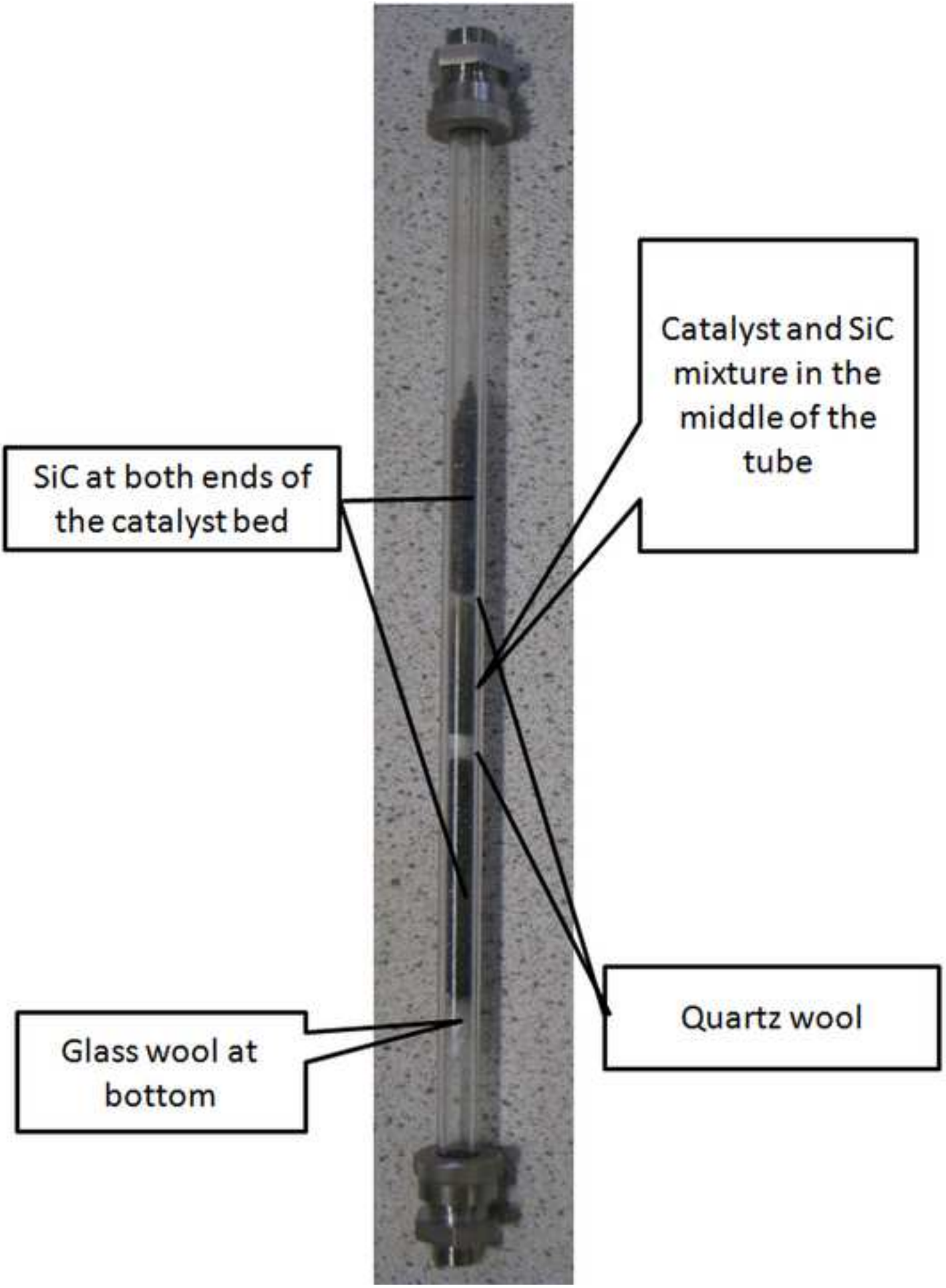

Figure 2

Click here to download high resolution image

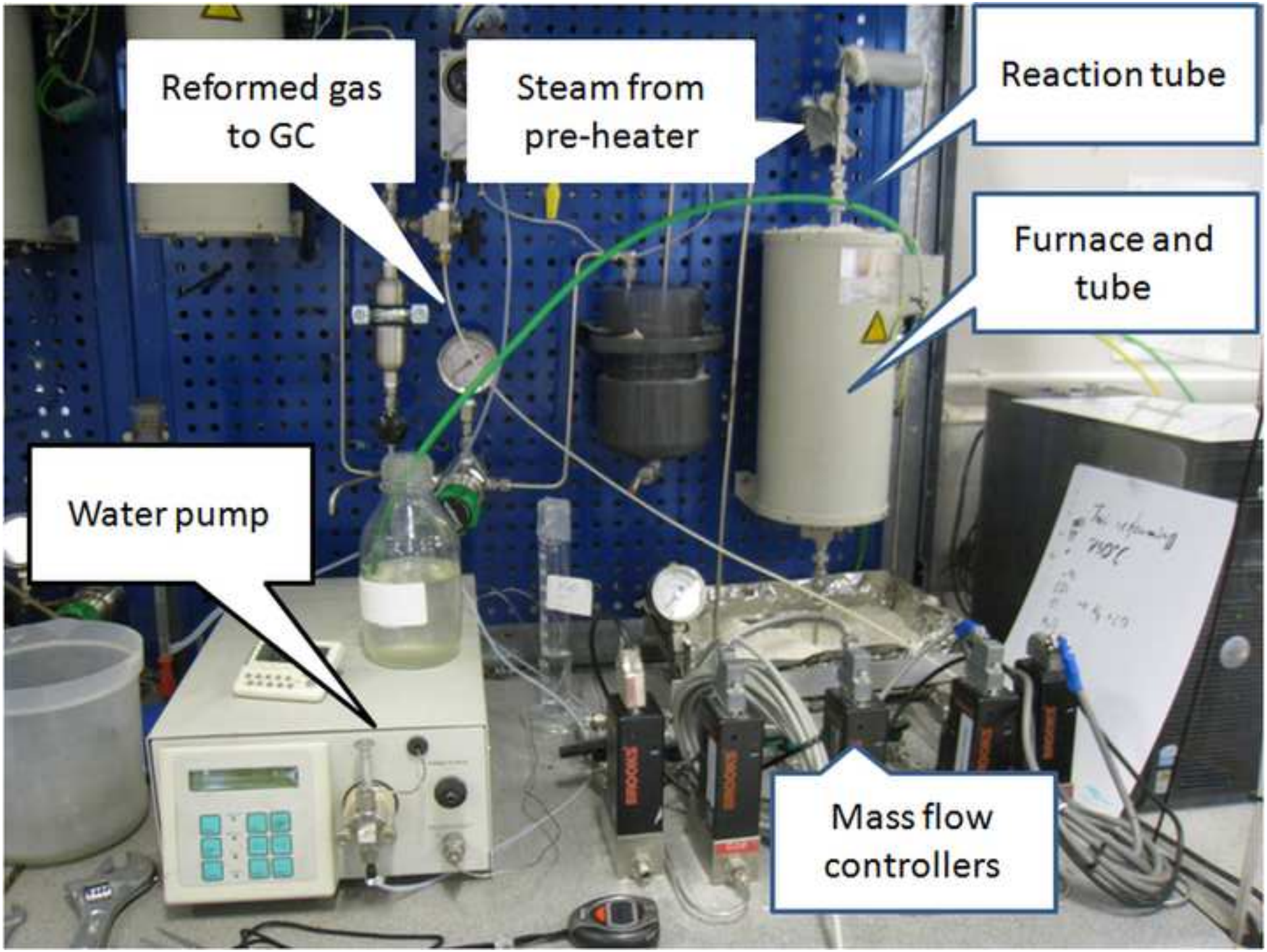

Figure 3

Click here to download high resolution image

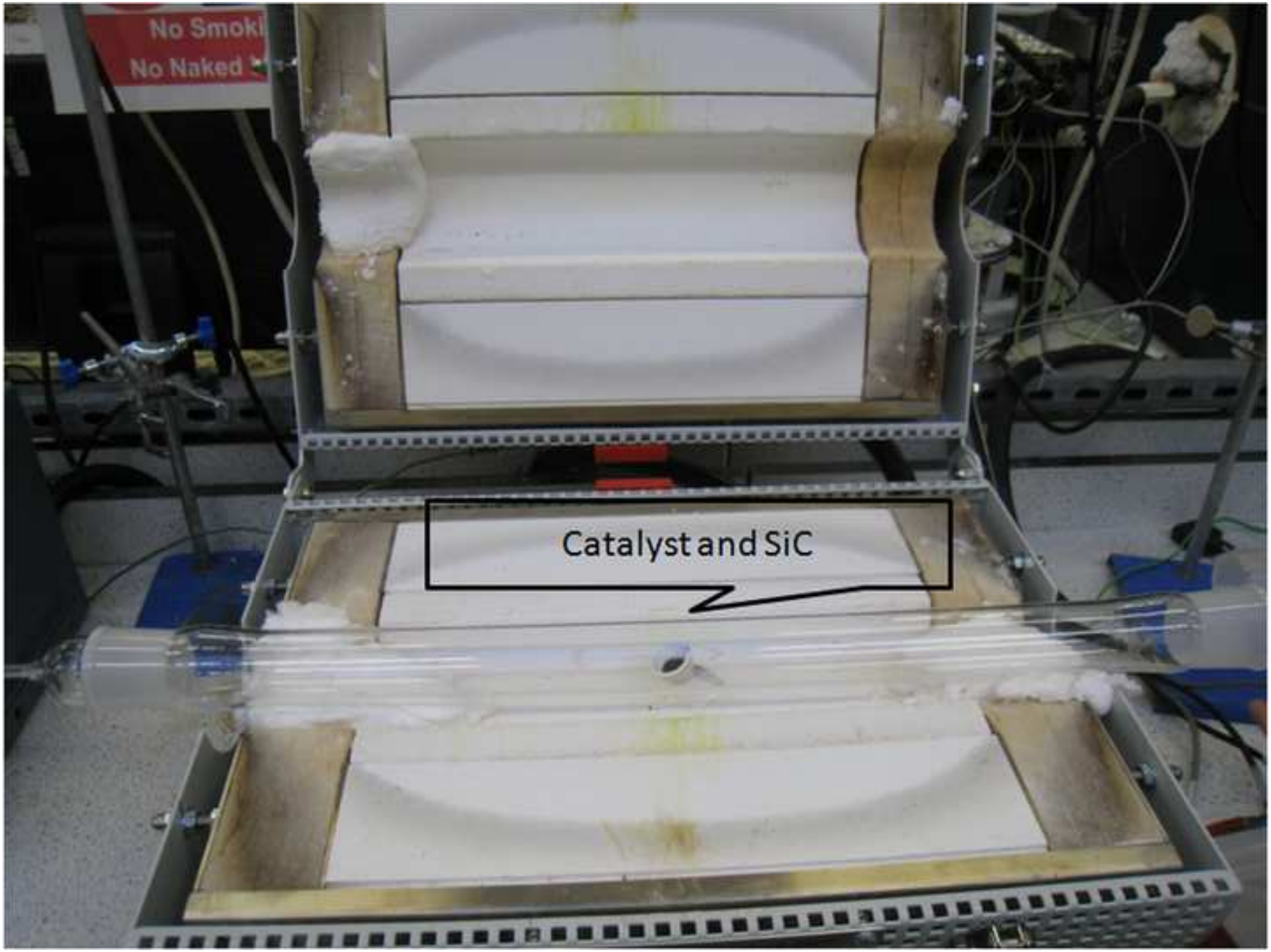

Figure 4
Click here to download high resolution image

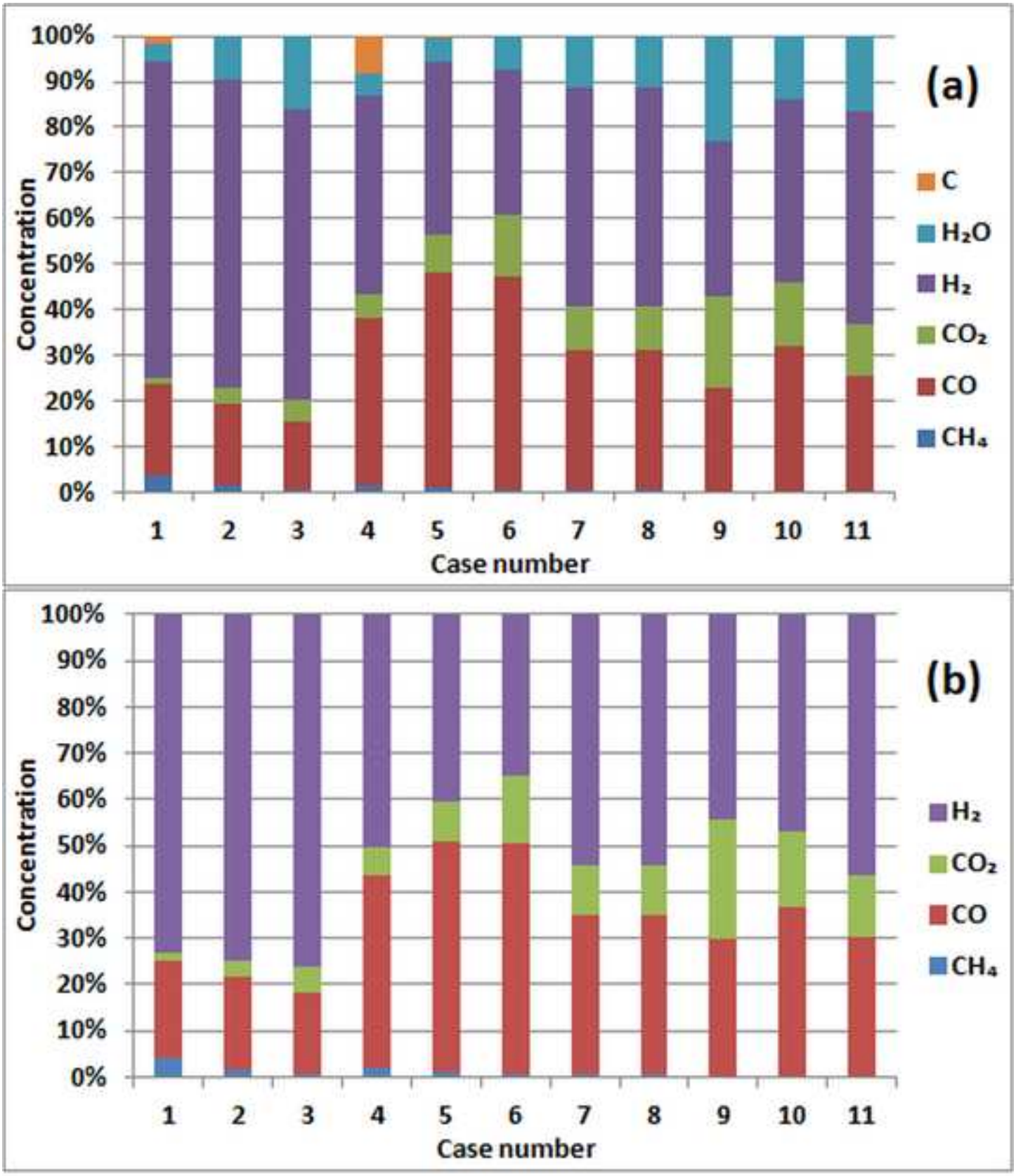

Figure 5

Click here to download high resolution image

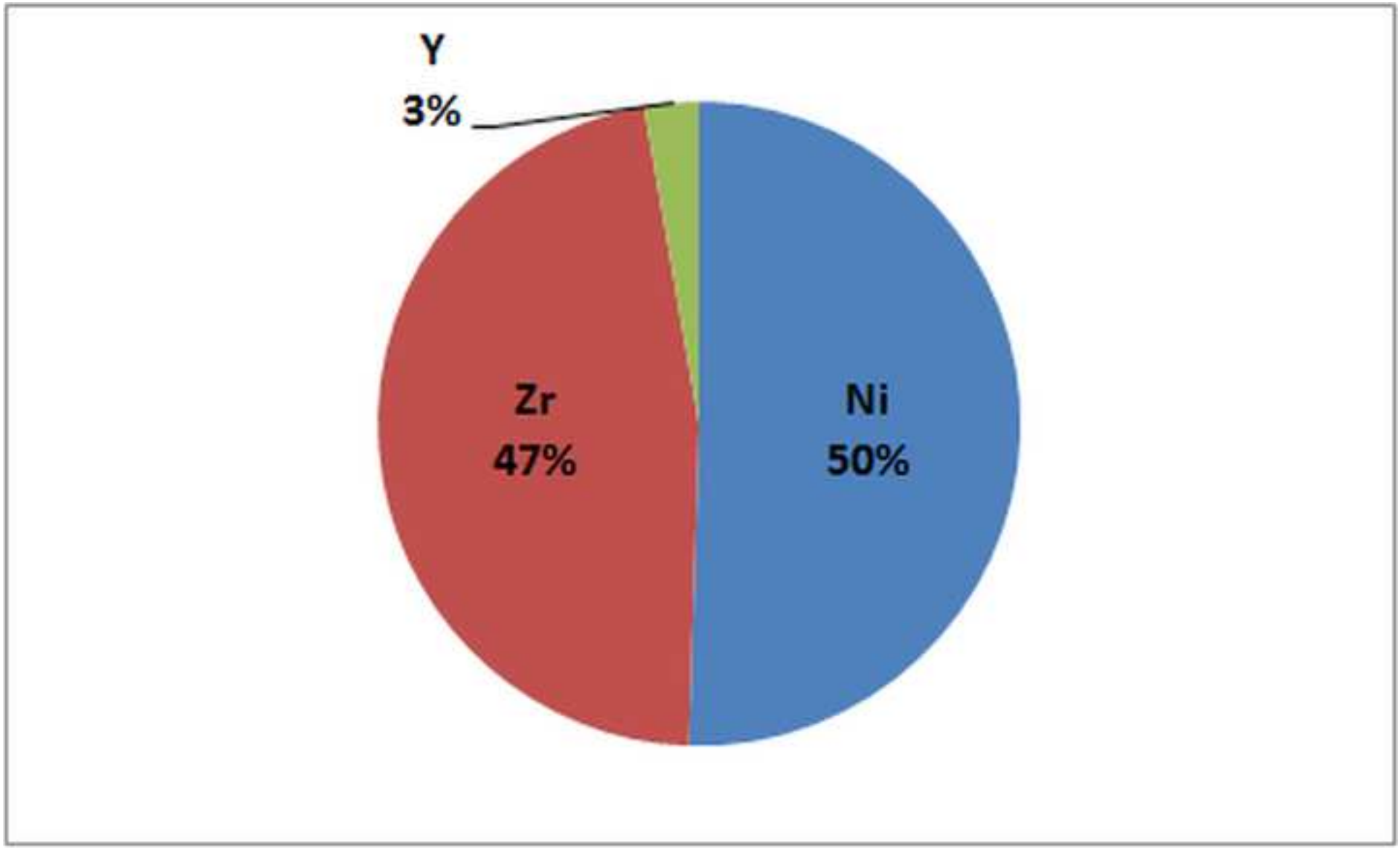

Figure 6

Click here to download high resolution image

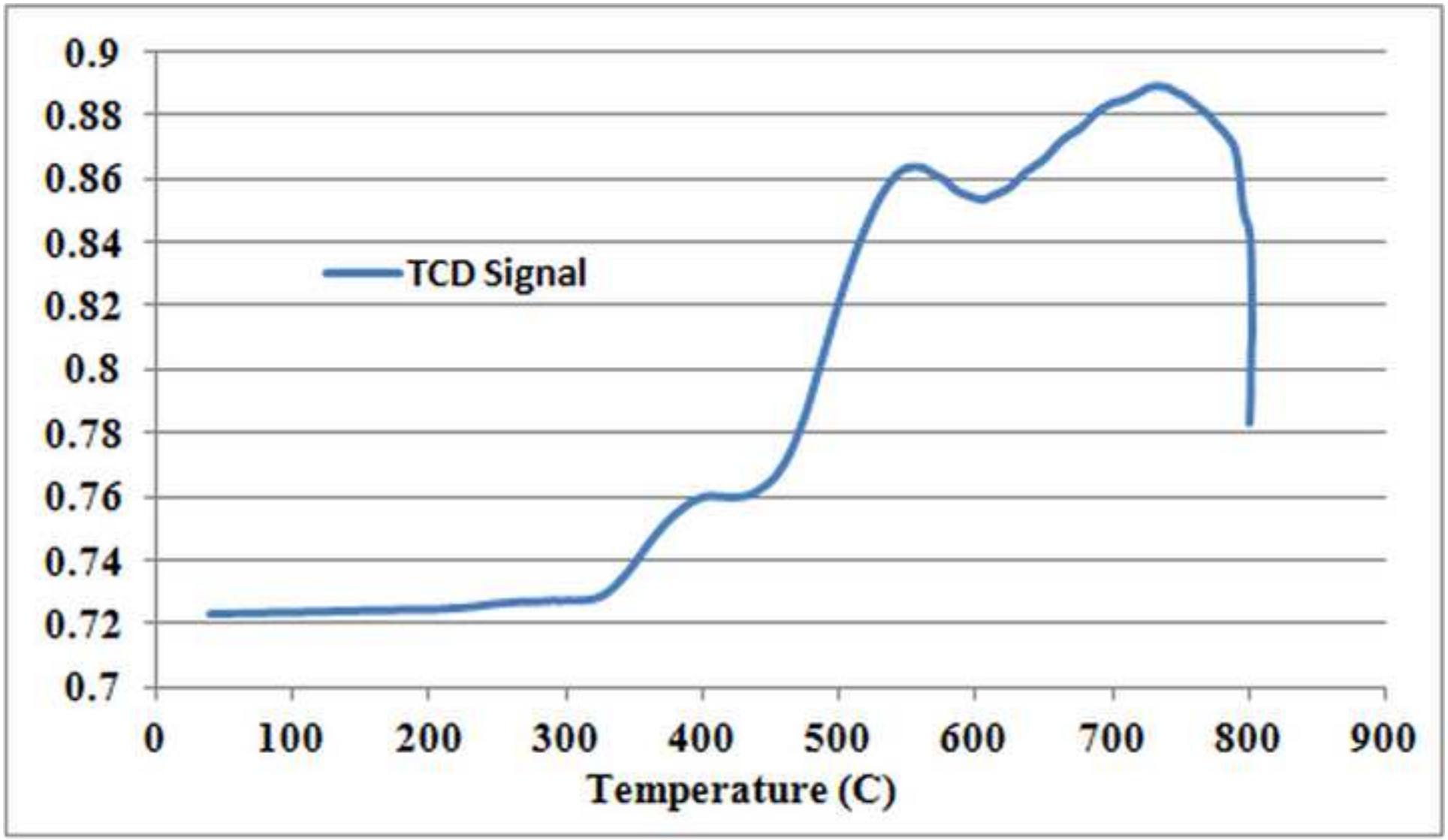

Figure 7

Click here to download high resolution image

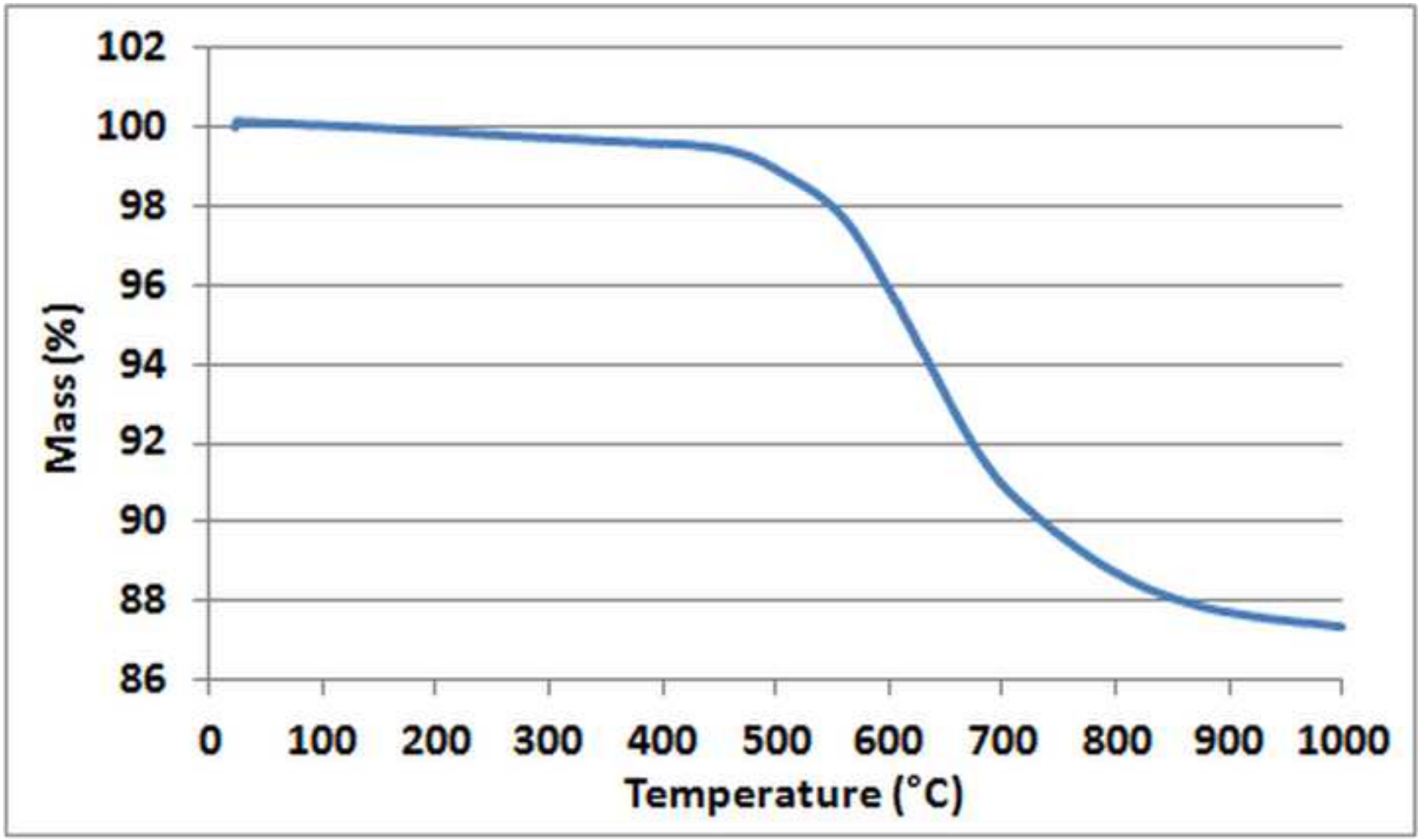

Figure 8

Click here to download high resolution image

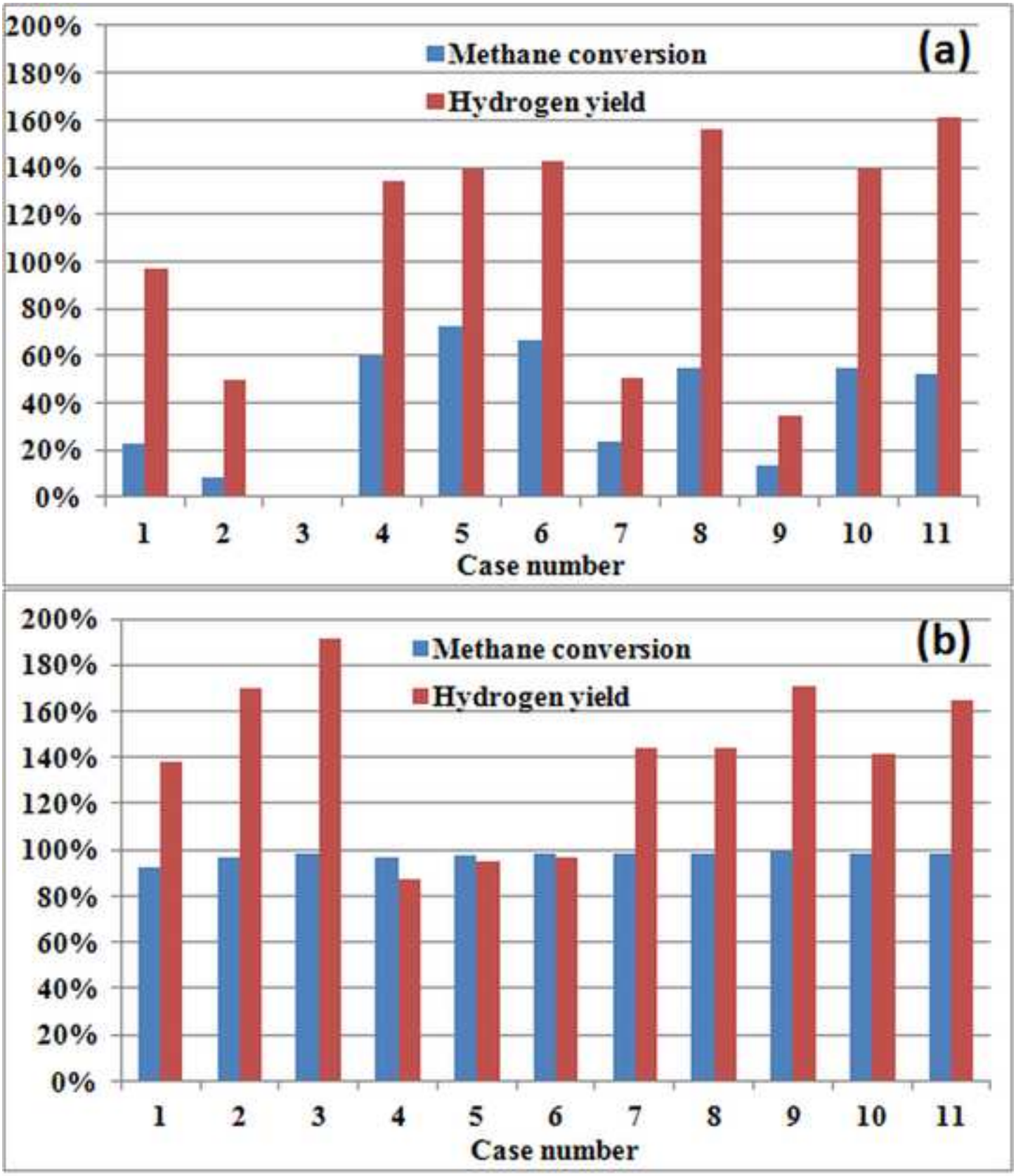

Figure 9
Click here to download high resolution image

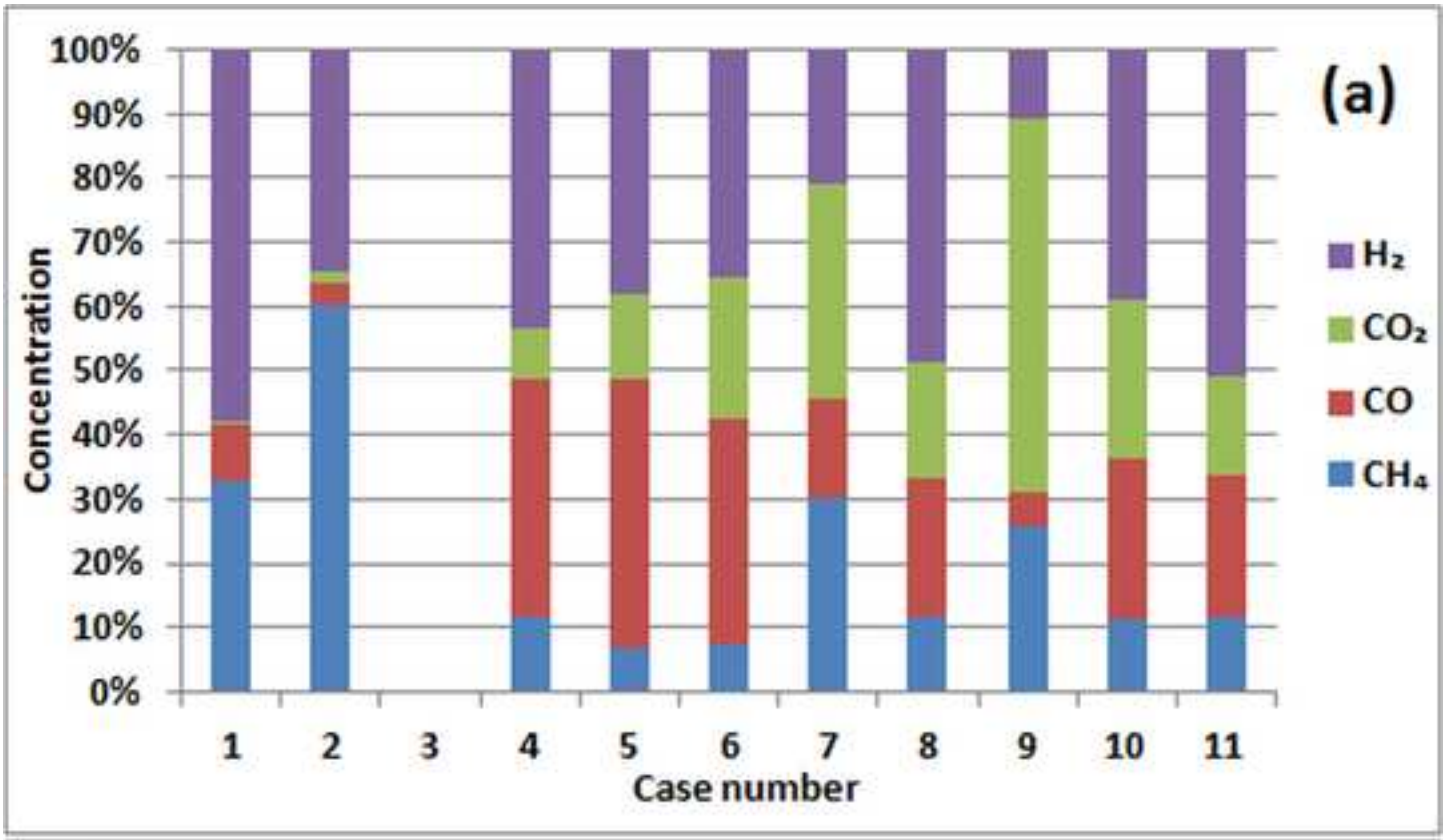

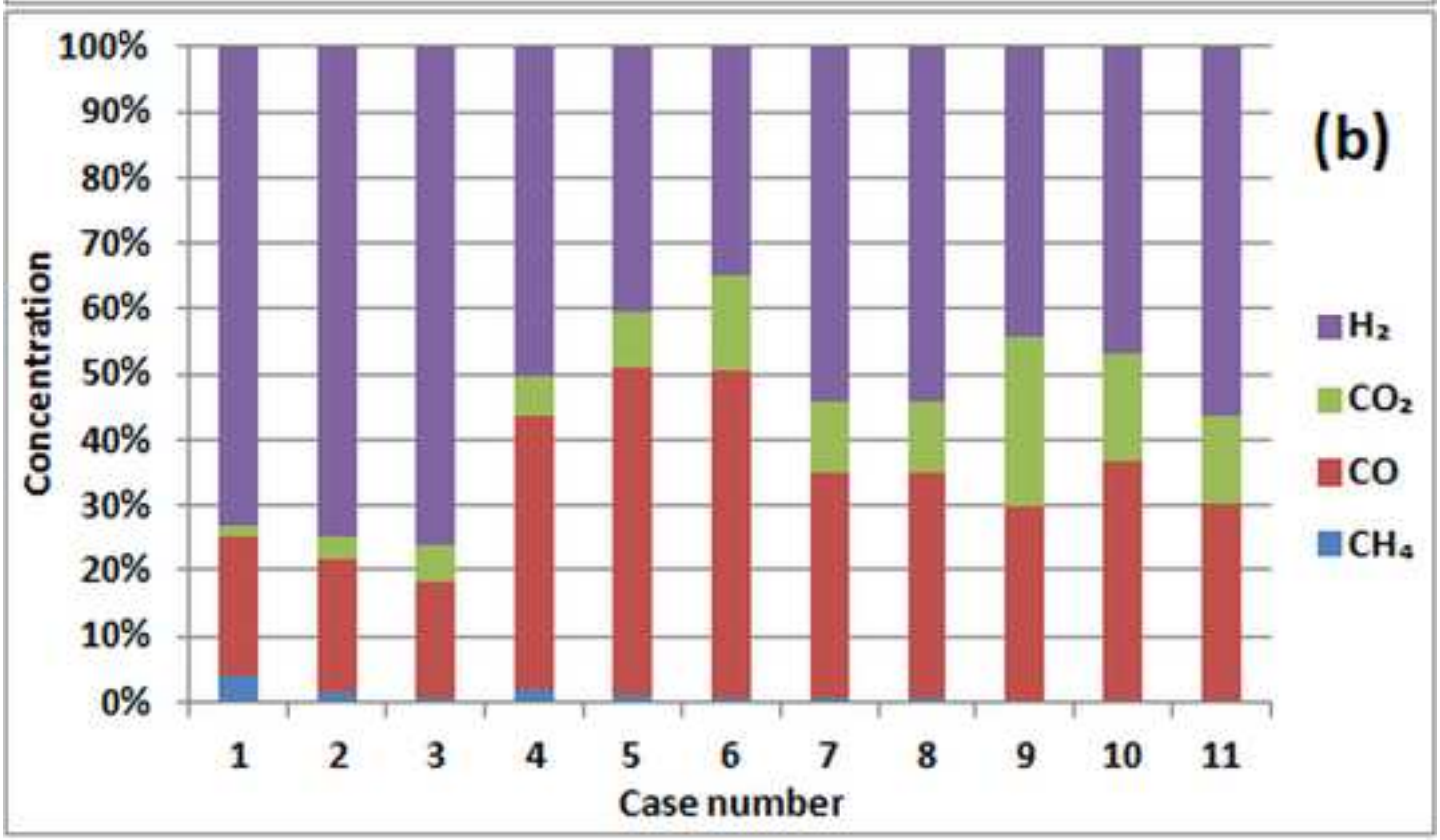

Figure 10
Click here to download high resolution image